Design of a Multi-Band, Dual-Sense Polarization Reconfigurable Mushroom Shape Patch Antenna

Renu Agrawal[1$*], Subhash Shrimal[2$], Bhawna Kalra[3$], M.M. Sharma[4$]

[$] Department of ECE, Malaviya National Institute of Technology, Jaipur, India

[1]*2019rec9553@mnit.ac.in, [2]2019rec9534@mnit.ac.in, [3] 2019rec9507@mnit.ac.in, [4]mms.ece@mnit.ac.in

*+91-7597899229

Abstract:

This manuscript unveils a novel approach to crafting a reconfigurable circularly polarized patch antenna, facilitating its operation across various frequency bands (ITS/WLAN/INSAT). The technique involves using a circular patch with defected ground having slotted symmetrical slits and two p-i-n diodes, which can switch between ON and OFF states to achieve far-field polarization reconfigurability among linear polarization (LP), right-hand circular polarization (RHCP), and left-hand circular polarization (LHCP). The antenna has been fabricated and shows good matching with the simulated results, indicating its potential for use in various wireless communication applications. The measured bandwidth ($|S_{11}|$<-10dB) of the proposed antenna is 19.81% and 10% for the two LP modes, while the 3dB axial ratio bandwidth spans 4.56% and 8.33% for the two CP modes. Within these two bands, circularly polarized radiation with opposite polarization states is achieved, aligning with the impedance matching band ($|S_{11}|$<-10dB). The designed antenna exhibits a peak gain of approximately 3.5 dBi and 2.9 dBi within the 3 dB axial ratio bandwidths in the lower and upper bands, respectively.

Keywords: Circular Patch Antenna, Circular Polarization, Dual-Sense, Multi-Band, Mushroom-Shape, Reconfigurable.

1. Introduction

The field of wireless communication has seen tremendous growth in recent epochs, culminating in the evolution of new and innovative communication frameworks [1-3]. Antennas are crucial in modern wireless technology, serving as conduits for seamless signal transmission [4]. Amidst this dynamic landscape, the integration of multiband and Circularly Polarized (CP) antennas has become indispensable [5], [6]. The diverse nature of wireless communication necessitates antennas capable of operating across various frequency bands, making multiband antennas vital for accommodating different signal ranges. This adaptability optimizes connectivity in an era characterized by myriad wireless devices. Circularly Polarized antennas, with their ability to mitigate signal distortion and enhance reception, have emerged as crucial components. Their unique polarization properties enable superior performance in environments with varying signal reflections, ensuring a stable and reliable connection. With the demand for different frequency bands, polarizations, and radiating characteristics, reconfigurable antennas capable of multiple functions with a single design are essential [7-10]. These antennas enhance signal quality, reduce interference, and offer increased flexibility, making them indispensable for modern wireless applications. The research domain for such antennas, encompassing various characteristics like frequency bands, polarizations, and radiations, is expansive and continuously evolving to meet the escalating demands of high-performance wireless communication systems [11-22]. Various types of reconfigurable antennas with multi-band circular polarization have been documented in the existing literature. In [11], an innovative miniaturized loop-based structure is explored for angular stability and polarization independence in a multiband band pass frequency selective surface designed for different wireless applications. In another work [12], an antenna designed for 5G systems is presented. Additionally, a comprehensive review titled multiband reconfigurable antennas for 5G wireless and Cube Sat applications is provided in [13] highlighting features with switchable slots and shorting posts for generating RHCP and LHCP.

Further research is reported in [14,15], investigating a frequency and pattern reconfigurable antenna, as well as an electrically adjustable antenna capable of multi-polarization reconfiguration, utilizing quadruple patches. In [16], a study on a frequency and polarization-reconfigurable corner truncated microstrip square patch antenna is presented. To address bandwidth limitations, [17] introduces a technique utilizing multiple resonances for increasing the bandwidth of reconfigurable antennas. The paper referenced in [18] explores a reflect array antenna designed for satellite usage within the Ku-band, featuring full reconfigurability and circular polarization across two frequency bands, while [19] delves into the design of an L/S multiband frequency-reconfigurable antenna tailored specifically for satellite applications. The utilization of circularly polarized modes is investigated in [20] to create a polarization-adaptable antenna.Versatile antennas capable of adjusting polarization and accommodating bidirectional communication over a broad frequency range with a switchable feeding network using multiple diodes and a reconfigurable antenna beam using a U-shaped slot patch for wireless networks are presented in [21-26]. In [25], a dual-band circularly polarized mushroom-shaped antenna is studied. This suggested antenna has a shape similar to our proposed one, but the proposed work in the manuscript presents the multiband operation with polarization reconfigurability, which makes it different from the antenna proposed in [25].

However, these innovative designs face certain limitations. For instance, integrating several diodes may lead to intricate DC-bias networks, complicating the implementation of the system. Providing independent bias for each diode can be challenging and might necessitate special mechanisms such as the use of capacitors. To tackle these challenges, the paper introduces a rudimentary monopole antenna featuring reconfigurable dual-band CP functionality. This antenna generates RHCP, LHCP, and LP across various frequency bands through a streamlined biasing network. The design overcomes the issues of the large number of diodes and the need for complex biasing networks. The antenna achieves reconfigurable polarization by using two p-i-n diodes positioned on the slits within the ground plane. By carving rectangular apertures along the bottom edges of the circular emitting patch, we enhance the resonance pathway, causing the resonance frequency to shift towards the lower end of the fundamental frequency spectrum for the radiator patch. The apertures disrupt the flow of surface currents, resulting in the emergence of two opposing CP bands when only one diode is activated, with one being LHCP and the other RHCP. Conversely, when the same diode is in the deactivated state, the surface currents shift, yielding two CP bands with opposite polarization compared to the activated state, i.e., one RHCP and one LHCP. Additionally, when both the p-i-n diodes are in their activated/deactivated state, they manifest two linearly polarized (LP) frequency bands. This design is suitable for applications such as C-band communication satellite uplink and downlink operations. The antenna's bandwidth is also suitable for wireless communication systems.

In Section 2, details regarding the setup, design methodology, operational mechanism, and characteristics of the proposed antenna are outlined. Section 3 illustrates the developmental phases and establishment of the antenna. The parametric analysis of the antenna is covered in Section 4. The manufacturing and laboratory testing of the suggested antenna is presented in Section 5. The simulation outcomes and their correlation with the experimental findings from the laboratory testing of the printed antenna are presented in Section 6. The final section, Section 7, encapsulates the derived conclusions from the study.

2. Antenna Design

2.1 Antenna Structure

The proposed circularly polarized mushroom-shaped microstrip-fed monopole antenna is a novel design simulated using CST software. The antenna uses a dielectric substrate of FR-4 material (ε_r=4.3) having a thickness of 1mm. The antenna receives input from a microstrip feed line with a characteristic impedance of 50 ohms. The antenna is comprised of a circular patch featuring rectangular slots, accompanied by a set of symmetrical slits integrated into a defective ground and augmented with a duo of p-i-n diodes. The circular patch is the main radiator of the antenna, while the slits loaded in the defective ground act as a reflector to enhance the antenna's performance. The diodes are used to switch the antenna's polarization states, which allows the antenna to operate in different polarizations.

The circularly polarized mushroom-shaped microstrip-fed monopole antenna presented in this paper is an efficient and compact design that offers polarization diversity, crafted to be adaptable across various uses, encompassing satellite communication, navigation, and wireless communication setups. The antenna's circular polarization offers an advantage over linear polarization, as it can help to reduce signal fading and improve the overall signal quality. For designing a circular patch antenna, the fundamental mode occurs at a resonance frequency whose wavelength corresponds to the perimeter of the circular patch that is given as [2]

$$F_r = \frac{C}{2\pi R_p\left(\sqrt{\varepsilon_{eff}}\right)} \qquad \text{………………………………………… (1)}$$

Where F_r is the fundamental frequency of the antenna, $2\pi R_P$ is the perimeter, C symbolizes the velocity of light when it traverses through a vacuum, and ε_{eff} denotes the effective permittivity.

From equation (1)

$$2\pi R_p = \frac{C}{F_r\sqrt{\varepsilon_{eff}}} \qquad \ldots\ldots\ldots\ldots\ldots\ldots\ldots\ldots\ldots\ldots\ldots\ldots\ldots\ldots (2)$$

Equation (2) shows that the resonance radius of the patch around the guided wavelength depends upon the effective permittivity of the dielectric. Monopole antenna typically generates linearly polarized radiations that are either vertical or horizontal. However, creating two perpendicular current elements of the same strength but with a 90-degree phase gap, which is necessary for circularly polarized radiation, can be challenging. To overcome this challenge, a perturbation segment can be introduced into an LP antenna to convert the perpendicular modes to LHCP /RHCP radiation. The proposed antenna design introduces perturbations in the antenna structure to achieve the desired CP radiation. This approach is a significant improvement over traditional methods that require multiple antennas and complex signal processing to attain CP. The suggested antenna design, as shown in Figure 1, is more compact and offers a simpler solution to achieving CP radiation. The specifications of the suggested antenna are presented in Table 1.

We have used Skyworks SMP1320-079LF silicon PIN diodes as RF-switching components to achieve polarization reconfigurability. In the CST simulation, Figure 2 (a) illustrates the diode represented as a series of low resistance (R = 4.7 Ω) and inductance (L = 0.15nH) when in the "ON" state. Conversely, Figure 2(b) illustrates the "OFF" state, approximated by combining (C= 0.017pF) and (R= 7KΩ) in parallel, with a series combination of inductance (L= 0.15nH) [27]. The essential part of the antenna setup is its biasing circuit, as shown in Figure 2(c). Each slot connects to a slender jumper wire through an RF choke, which includes a labeled inductor as L_b with a value of 68nH. The direct current bias lines are connected to the terminals of the PIN diode, facilitating the soldering of wires for battery connection [24].

3. Development Stages of the Proposed Antenna

To achieve a polarization reconfigurable antenna, the proposed antenna design is evaluated in four steps, labelled Ant1, Ant2, Ant3, and Ant4, as shown in Figure 3. In the first three steps, a circularly polarised antenna is designed, and finally, in step 4, a reconfigurable antenna is designed. In the first step, Ant1 is designed as a circular metallic patch antenna that resonates at a frequency of 6.3GHz and excites TM11 mode. This structure is created by etching a circular metallic patch with a radius R_p onto the upper surface of a dielectric substrate FR 4. The resonance radius used in the proposed antenna is R_p=5 mm. The obtained impedance bandwidth (IBW) for Ant1 is 5.38GHz-8.24 GHz, as shown in Figure 4 (a). The IBW of Ant1 shows that it is a well-designed circular patch antenna with good performance and wide bandwidth with its linear polarization ability.

In the next step, Ant1 is modified, and the defect is introduced in Ant2. Ant2 implements a simple, effective technique to alter the polarization state and generate circularly polarized waves. The approach involves introducing an L-slot in the rectangular ground of Ant1 along the -X direction to produce two orthogonal electric field vectors with equal magnitude and 90° phase difference. By optimizing the length of the slot, the antenna generates a CP mode at a frequency of 6.2 GHz. The simulation results of IBW and 3 dB ARBW for Ant2 are shown in Figures 4 (a) and 4(b), respectively. In step 3, Ant2 is modified and presented as Ant3 to achieve the desired impedance bandwidth. Impedance matching is attained by creating two symmetrical rectangular slots with dimensions $S_x \times S_y$ on the patch, thereby augmenting the antenna's performance. Additionally, in Ant3, we have introduced a vertical slit adjoining the L-slot, which creates the second CP band at a frequency of 4.5GHz. With the proposed modifications, the higher band of the S_{11} curve shifts towards the desired lower frequency and provides proper impedance matching within the CP bands. The simulated results, as depicted in Figure 4(a), observe that the impedance bandwidth for

Ant3 is 4.3GHz-4.88GHz with a center frequency of 4.5 GHZ and 5.16GHz-7GHz at the center frequency of 6.2GHz for lower and upper bands, respectively. The 3-dB axial ratio bandwidth for Ant3, as shown in Figure 4(b), is estimated to be 4.5GHz-4.71GHz and 5.7GHz-6.2GHz for lower and upper-frequency ranges, respectively. The circular polarization of Ant3 makes it an ideal choice for applications that require stable communication even when the antenna is not precisely oriented.

The Ant3 is modified and defect is introduced in the ground plane to achieve the reconfigurability. The final prototype is presented as Ant4. The strengths of Ant2 and Ant3 are combined to obtain Ant4. The mirror image is introduced in the +X direction for polarization reconfigurability. This proposed antenna (Ant4) offers unparalleled polarization diversity, making it a versatile and efficient option for a diverse array of uses. A prominent characteristic of Ant4 is the use of two switching diodes placed on the ground surface. This design enables the antenna to quickly and easily switch between different polarization states, allowing it to adapt to changing conditions and environments. The simulated results for IBW and ARBW of Ant4 are shown in Figure 5 (a) and (b), respectively.

The obtained IBW and ARBW are showcased in Table 2, which demonstrates the impressive functioning of the antenna across a range of different states. It is evident from Table 2 that when Diodes D1 and D2 are either OFF or ON, linear polarization is obtained. While one of the Diodes is ON and the other is OFF, circular polarization is achieved because two orthogonal electric field vectors with equal magnitude and 90° phase difference are generated. Hence, by switching the positions of diodes, the reconfigurability of polarization is achieved. Overall, the combination of advanced technology and cutting-edge engineering makes the proposed antenna Ant4 a powerful and effective tool for various applications, and its versatile polarization diversity means that it can adapt to even the most challenging of environments.

The graph in Figure 6 (a) and (b) illustrates the surface current patterns of the proposed antenna at frequencies of 4.5GHz and 6.2GHz, respectively. This is observed when D1 is activated, and D2 is deactivated. At the resonance frequency of 4.5GHz, the surface current rotates counter clockwise, resulting in RHCP radiation in the positive Z-direction. Conversely, at 6.2GHz, the surface current rotates clockwise, yielding LHCP radiation in the positive Z-direction. By reversing the switching state (D1 deactivated and D2 activated) of diodes, the sense of polarization changes from RHCP to LHCP and vice versa. Due to the symmetry of the design, here, we are presenting the results of the surface current patterns for the D1 ON and D2 OFF conditions of diodes.

4. Parametric Analysis

To evaluate the influence of optimized parameters on the operation of the proposed reconfigurable antenna (Ant 4), the dimensions of the rectangular slots and slits are investigated. One parameter out of the three slit lengths S_a, S_b, and S_c is changed at a time while keeping other parameters constant, aiming to observe the effects on impedance bandwidth and axial ratio. In the design of a proposed reconfigurable antenna, when diode D1 is activated while diode D2 remains inactive, and the lengths of the slits S_a, S_b, and S_c are sequentially adjusted, the outcomes are illustrated in Figure 7(a, b, c) and Figure 8(a, b, c) for IBWs and ARBWs, respectively. In these figures, we have incremented the length of the slits S_a, S_b, and S_c (one parameter at a time) by 0.2mm. This results in shifting of the lower and upper operational bands of frequency. This is due to the effect of change in the current length distribution path. It is demonstrated from the figures that the required IBW and 3-dB ARBW are obtained for corresponding values of S_a=2.4mm, S_b=5mm, and

S_c=2mm. Hence, these values are chosen to design the proposed antenna in this work. Results are the same if the switching states of the diodes (D1 made inactive and D2 activated) are reversed; due to the symmetry of the design, the results are not shown in the figure.

5. Antenna Fabrication and Measurements

The fabricated antenna is shown in Figure 9, along with the switching circuit for p-i-n diodes. The antenna is tested in an anechoic chamber. In the fabricated antenna, bias voltages play a crucial role in activating and deactivating the diodes responsible for polarization diversity. The diode assumes an active state in the absence of bias, transitioning to an inactive state upon the application of bias voltage. Conversely, the slotted slits structure within the DGS exhibits an open circuit configuration on the upper side when devoid of bias voltage, transforming into a closed circuit when subjected to bias voltage. The specifications for the antenna were obtained through the design process, as explained in section 4. The creation of the antenna in the laboratory involved employing a combination of photolithography and etching methods, with FR-4 serving as the dielectric material. The design of the antenna was crafted through computer simulations, focusing on enhancing its performance to the fullest extent. Precision was maintained throughout the fabrication process to guarantee the antenna's compliance with the specified requirements. To evaluate its effectiveness, various testing methods, including measurements of ARBW and return loss, were conducted. The outcomes revealed that the antenna not only met the desired specifications but also operated efficiently across frequency bands.

6. Results and Discussions

The examination of polarization diversity in the engineered antenna involves analyzing the simulated outcomes of IBW and ARWB utilizing CST software. In Figure 10, the measured and simulated IBW of the suggested antenna utilizing different operational modes of p-i-n diodes is represented. The IBW obtained when only one diode is kept ON is 4.3GHz-4.88GHz and 5.16GHz-7GHz for the frequency ranges at the bottom and top ends, correspondingly. Similarly, the ARBW of the designed antenna in different switching modes of the diodes is illustrated in Figure 11. The figures depict the ARBW obtained when only one diode is in an active state, 4.5GHz-4.71GHz and 5.7GHz-6.2GHz, respectively, for lower and upper bands. Examination of the figures reveals a consistent alignment between the simulated and measured results. Any slight disparities observed can be attributed to potential errors introduced during the fabrication process. Figure 12 represents the simulated and measured results for IBW when both the diodes are either in the OFF state or in the ON state. The IBW obtained is 4.9GHz-5.95GHz and 3.8GHz-4.4GHz GHz for both diodes ON and OFF, respectively. It is evident from the figure that the simulated and measured results closely match each other.

The variation of the simulated and measured gain of the proposed antenna is illustrated in Figure 13. Figure 13(a) shows that the antenna gain varies over 3.2-3.48 dBi and 2.86-2.93 dBi within 3-dB AR bandwidths for the lower and upper CP bands, respectively. The antenna gain varies from 3.5 to 3.8 dBi when switched to LP sense, as shown in Figure 13(b).

The simulated and quantified far-field radiation pattern of the suggested antenna is represented in Figure 14 at frequencies 4.5GHz and 6.2GHz when swapped to two CP bands. The figure depicts that the simulated and measured results closely match each other and have good broadside (+z direction) patterns for both E(x-z) and H(y-z) planes. It is also seen from the figures that while diode D2 is activated and D1 is deactivated, the lower band gives LHCP, and RHCP is obtained for the upper band. On the other hand, if we reverse the switching states of the diodes, the polarization state changes from LHCP to RHCP and vice versa for the lower and upper bands, respectively. Due to the design's symmetry, the results remain the same with reverse switching;

only the polarity changes, so they are not shown in the figures. Figure 15 depicts the simulated and measured radiation pattern of the proposed antenna at 5.3GHz and 4.2GHz when switched to LP mode. In both figures 15(a) and 15(b), the measure results of the theta-polarized are well agreed with the simulated ones. As for measurements, their phi-polarized values are slightly greater than those of the simulated ones due to cross-polarization of signal strength and measurement system errors. As expected, the LP mode shows a bi-directional radiation pattern in the E-plane and an omnidirectional pattern in the H-plane.

The comparison of this work with other similar work is given in Table 3. It is observed from the table that our designed antenna has a smaller size, less complex, and wideband characteristics in comparison to the other work mentioned in the table. The proposed antenna also uses only two p-i-n diodes to achieve polarization diversity.

7. Conclusions

In this paper, we have proposed and designed a mushroom-shaped multi-band dual-sense reconfigurable polarization antenna with small dimensions. The suggested antenna was printed and tested in the laboratory, and the results showed that the simulation and measured results closely matched. The antenna provides LP, RHCP, and LHCP by employing diverse switching modes of p-i-n diodes. In the OFF and ON state of the diodes, the designed antenna exhibits linear polarization with an IBW(S_{11}<-10dB) of 19.81%(4.3GHz-4.88GHz) and 10% (5.16GHz-7GHz,6.2 GHz). When either of the diodes is in the active state, the antenna demonstrates dual circular polarization bands with an ARBW(<3dB) of 4.56%(4.5GHz-4.71GHz) and 8.33%(5.7GHz-6.2GHz). Furthermore, the results include variations in antenna gain, featuring a maximum gain of 3.5 dBi in the lower frequency range and 2.9 dBi in the higher frequency range, within their respective 3-dB axial ratio bandwidths. The designed antenna is suitable for applications in C-band communication satellite uplink and downlink operations.

References

[1] Jin, G., Li, L., Wang, W., et al. "Broadband polarisation reconfigurable antenna based on crossed dipole and parasitic elements for LTE / sub-6 GHz 5G and WLAN applications", *IET Microwaves Antennas Propag.*, **14**(12), pp. 1469–1475 (2020). https://doi.org/10.1049/iet-map.2019.1137.

[2] Zhang, Z., Li, M., Dai, Q., et al. "Compact wideband dual-band polarization and pattern diversity antenna for vehicle communications", *IEEE Trans. Antennas Propag.*, **71**(5), pp. 4528–4533 (2023). DOI:10.1109/TAP.2023.3243855.

[3] Shankar, S. and Upadhyay, D.K. "A fractal monopole antenna with dual polarization reconfigurable characteristics for X-Band applications", *IEEE Access*, **11**, pp. 95667–95680 (2023). DOI: 10.1109/ACCESS.2023.3311133.

[4] Jhajharia, T., Tiwari, V., and Bhatnagar, D. "Polarisation reconfigurable dual-band circularly polarised patch antenna with defected ground plane for C-band wireless applications", *IET Microwaves Antennas Propag.*, **13**(14), pp. 2551–2558 (2019). https://doi.org/10.1049/iet-map.2018.6214

[5] Shukoor, M.A. "Wideband reconfigurable linear-linear and linear-circular polarizer / reflector integrated with RF PIN diodes for X / Ku / Ka-Band applications", *IEEE Wirel. Antenna Microwave Symposium*, Ahmedabad, India, pp. 1–5 (2023). DOI:10.1109/WAMS57261.2023.10242908.

[6] Melendro-Jimenez, J., Sanchez-Olivares, P., Tamayo-Dominguez, A., et al. "3D printed directive beam-steering antenna based on gradient index flat lens with an integrated

polarizer for dual circular polarization at W-Band", *IEEE Trans. Ant. and Propag.*, **71**(1), pp. 1059-1064 (2023). DOI: 10.1109/TAP.2022.3217177.

[7] Kumar, P., Dwari, S., and Saini, R.K., et al. "Dual-band dual-sense polarization reconfigurable circularly polarized antenna", *IEEE Antennas Wirel. Propag. Lett.*, **18**(1), pp. 64-68 (2019). DOI: 10.1109/LAWP.2018.2880799.

[8] Lv, X.L., Wu, B., Fan, C., et al. "Polarization/Frequency hybrid reconfigurable microstrip antenna utilizing graphene-based tunable resistor", *IEEE Antennas Wirel. Propag. Lett.*, **22**(2), pp. 367–371 (2023). DOI: 10.1109/LAWP.2022.3212885.

[9] Zhang, L., Sun, Y., He, Y., et al. "A quad-polarization reconfigurable antenna with suppressed cross polarization based on characteristic mode theory", *IEEE Trans. Antennas and Propagation.*, **69**(2), pp. 636–647 (2021). DOI: 10.1109/TAP.2020.3016384.

[10] Saraswat, K., and Harish, A. R. "Dual-band polarization reconfigurable grounded fractal slot antenna", *IET Microwaves Antennas Propag.*, **14** (14), pp. 1786–1790 (2020). https://doi.org/10.1049/iet-map.2020.0542

[11] Garg, J., Yadav, S., and Sharma, M.M. "A novel miniaturized loop based angularly stable and polarization independent multiband bandpass FSS structure for Wi-Max and WLAN applications", *Sadhana-Acad. Proc. Eng. Sci.*, **48**(1), pp. 1-7 (2023). https://doi.org/10.1007/s12046-022-02068

[12] Al Muttairi, A.I., and Farhan, M.J. "Circular polarization reconfigurable antenna for mid-band 5G applications with a new reconfigurable technique", *Indones. J. Electr. Eng. Comput. Sci.*, **19**(2), pp. 802–810 (2020). https://doi.org/10.11591/ijeecs.v19.i2.pp802-810.

[13] Ramahatla, K., Mosalaosi, M., Yahya, A., et al. "Multiband reconfigurable antennas for 5G wireless and cubesat applications", *IEEE Access.*, **10,** pp. 40910–40931 (2022). DOI:

10.1109/ACCESS.2022.3166223.

[14] Karthika, K., and Kavitha, K. "Design and development of parasitic elements loaded quadband frequency and pattern reconfigurable antenna", *Int. J. RF Microw. Comput. Eng.*, pp. 1-10 (2023). https://doi.org/10.1155/2023/4034241.

[15] Li, M., Zhang, Z., and Tang, M.C. "A compact, low-profile, wideband, electrically controlled, tri-polarization-reconfigurable antenna with quadruple gap-coupled patches", *IEEE Trans. Antennas Propag.*, **68**(8), pp. 6395–6400 (2020). DOI: 10.1109/TAP.2020.2970073.

[16] Anantha, B., Merugu, L., and Rao, S.P.V.D. "A novel single feed frequency and polarization reconfigurable microstrip patch antenna", *Int. J. Electron. Commun.*, **72,** pp. 8–16 (2017). https://doi.org/10.1016/j.aeue.2016.11.012

[17] Li, M., Zhang, Z., Tang, M.C., et al. "Bandwidth enhancement and size reduction of a low-profile polarization-reconfigurable antenna by utilizing multiple resonances", *IEEE Trans. Antennas Propag.*, **70**(2), pp. 1517–1522 (2022). DOI: 10.1109/TAP.2021.3111309.

[18] Baladi, E., Xu, M.Y., Faria, N., et al. "Dual-band circularly polarized fully reconfigurable reflectarray antenna for satellite applications in the Ku-band", *IEEE Trans. Antennas Propag.*, **69** (12), pp. 8387–8396 (2021). DOI: 10.1109/TAP.2021.3090577.

[19] Sun, M., Zhang, Z., Zhang, F., et al. "L/S multiband frequency-reconfigurable antenna for satellite applications", *IEEE Antennas Wirel. Propag. Lett.*, **18**(12), pp. 2617–2621 (2019). DOI: 10.1109/LAWP.2019.2945624.

[20] Wang, S., Yang, D., Geyi, W., et al. "Polarization-reconfigurable antenna using combination of circular polarized modes", *IEEE Access.*, **9**, pp. 45622–45631 (2021). DOI: 10.1109/ACCESS.2021.3067064.

[21] Liu, M., Zhai, Z.J., Lin, F., et al. "Wideband quad-polarization-reconfigurable bidirectional antenna with a simple wideband switchable feeding network", *IEEE Antennas Wirel. Propag. Lett.*, **22**(6), pp. 1346–1350 (2023). DOI: 10.1109/LAWP.2023.3241987.

[22] Suriyan, K., Ramalingam, N., and Venusamy, K. "Reconfigurable antenna beam using U-shaped slot patch for wireless networks", *Mater. Today Proc.*, **58**, pp. 547–551 (2022). https://doi.org/10.1016/j.matpr.2022.03.063.

[23] Shaw, M., and Choukiker, K.Y. "Analysis of frequency reconfigurable microstrip patch antenna with unidirectional radiation pattern for IRNSS band", *Int. J. Electron. Commun.*, **141** (2021). https://doi.org/10.1016/j.aeue.2021.153962.

[24] Shaw, M., and Choukiker, K.Y. "Reconfigurable polarization and pattern microstrip antenna for IRNSS band applications", *Int. J. Electron. Commun.*, **160** (2023). https://doi.org/10.1016/j.aeue.2022.154501

[25] Kumar, Y., Gangwar, R.K., and Kanaujia, B.K. "Characterization of dual-band circularly polarized mushroom-shaped monopole antenna with modified ground plane", *Frequenz.*, **77**(1-2), pp. 39-51 (2023). https://doi.org/10.1515/freq-2022-0002.

[26] Tran, H.H., Nguyen, T.N., and Abbosh, A.M. "Simple design procedure of a broadband circularly polarized slot monopole antenna assisted by characteristic mode analysis", *IEEE Access.*, **6**, pp. 78386-93 (2018). DOI: 10.1109/ACCESS.2018.2885015.

[27] Shrimal, S., Sharma, I.B., Kalra, B., et al. "A Compact Ground-slitted CPW-fed Polarization Reconfigurable Antenna for Wireless LAN applications", *IEEE Int. Conf.* on *Microwave Antennas Propag. (MAPCON),* Bangalore, India, pp. 1393-1397 (2022). DOI: 10.1109/MAPCON56011.2022.10047383.

Figure Captions

Figure 1: Configuration of the suggested antenna (a) Top view (b) Rear view

Figure 2: Equivalent circuit of p-i-n diode (a) ON condition (b) OFF condition (c) Biasing circuit

Figure 3. Evolution steps of the suggested antenna

Figure 4: Simulated results for Ant1, Ant2, and Ant3 (a) Impedance Bandwidth (b) Axial Ratio

Figure 5: Simulated results of antenna 4 for different states of diodes (a) Impedance Bandwidth (b) Axial Ratio

Figure 6: Simulated surface current distribution of proposed antenna 4 at (a) 4.5 GHz (RHCP) and (b) 6.2 GHz (LHCP) with diode switching states as D1=ON & D2=OFF.

Figure 7: Simulated Impedance Bandwidth of antenna 4 for different values of (a) slit length S_a (b) slit length S_b (c) slit length S_c for D1=ON/OFF &D2=OFF/ON.

Figure 8: Simulated Axial Ratio bandwidth of antenna 4 for different values of (a) slit length S_a (b) slit length S_b (c) slit length S_c for D1=ON/OFF &D2=OFF/ON.

Figure 9: (a) Antenna with biasing circuit (b) Testing of the suggested antenna in the anechoic chamber

Figure 10: Evaluation of simulated and measured S_{11} for different p-i-n diodes switching states of the suggested antenna

Figure 11: Simulated and measured Axial ratio bandwidth for various switching modes

Figure 12: Comparison of simulated and measured IBW of the proposed antenna when both diodes are simultaneously OFF and ON

Figure 13: Comparison of simulated and measured Gain of the designed antenna for different switching states of the diodes (a) D1=ON&D2=OFF/ D1=OFF&D2=ON (b) D1D2=ON/D1D2=OFF

Figure 14: Simulated and measured radiation pattern of the proposed antenna (a) at 4.5GHz (b) at

6.2 GHz with diode switching D1=OFF& D2=ON when at working as LHCP & RHCP

Figure 15: Simulated and measured radiation pattern of the proposed antenna (a) at 5.3GHz (b) at 4.2 GHz with diode switching D1=ON & D2=OFF

Table Captions

Table 1 Specifications for the suggested antenna's parameters

Table 2 Performance of the suggested antenna for various switching modes of p-i-n diodes

Table 3 Comparative study of the proposed antenna with earlier designed dual band antennas

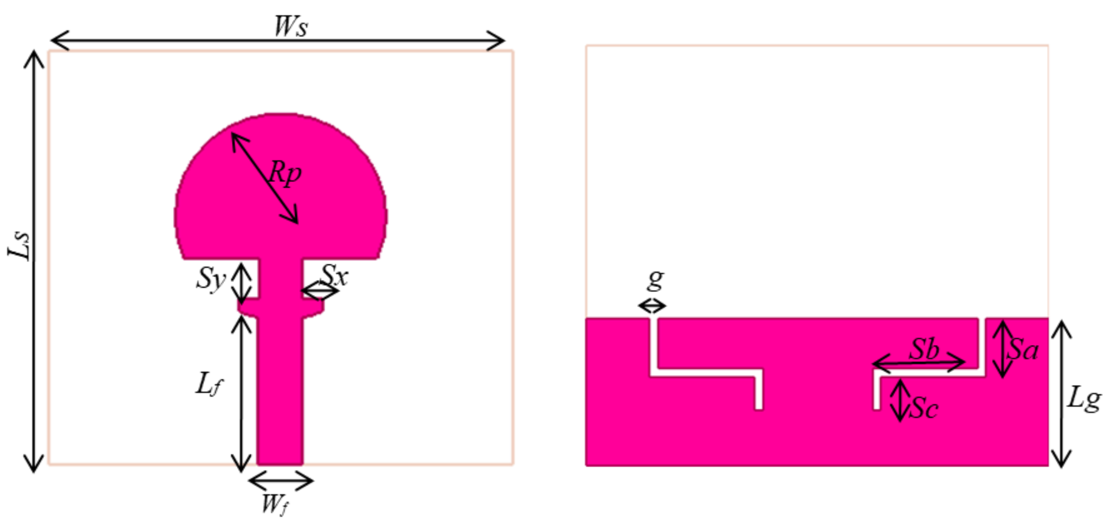

(a) (b)

Figure 1: Configuration of the suggested antenna (a) Top view (b) Rear view

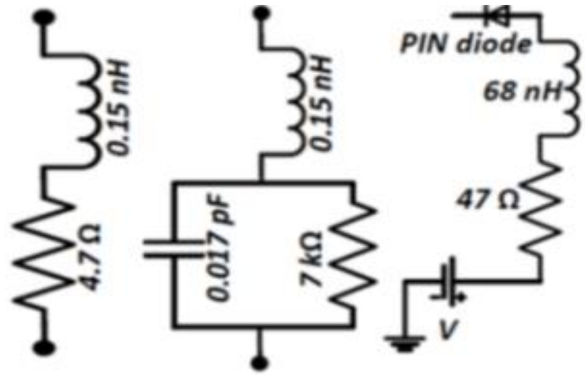

(a) (b) (c)

Figure 2: Equivalent circuit of p-i-n diode (a) ON condition (b) OFF condition (c) Biasing circuit

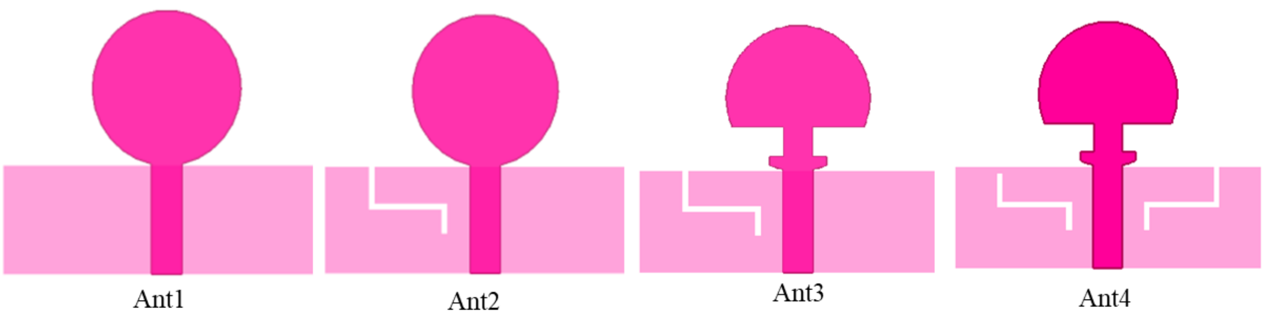

Figure 3. Evolution steps of the suggested antenna

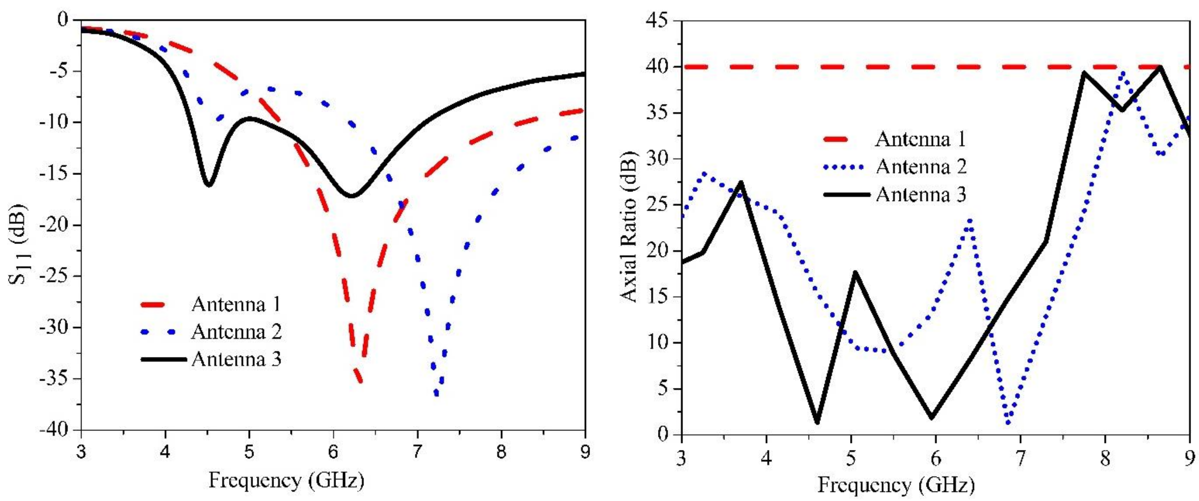

(a) (b)

Figure 4: Simulated results for Ant1, Ant2, and Ant3 (a) Impedance Bandwidth (b) Axial Ratio

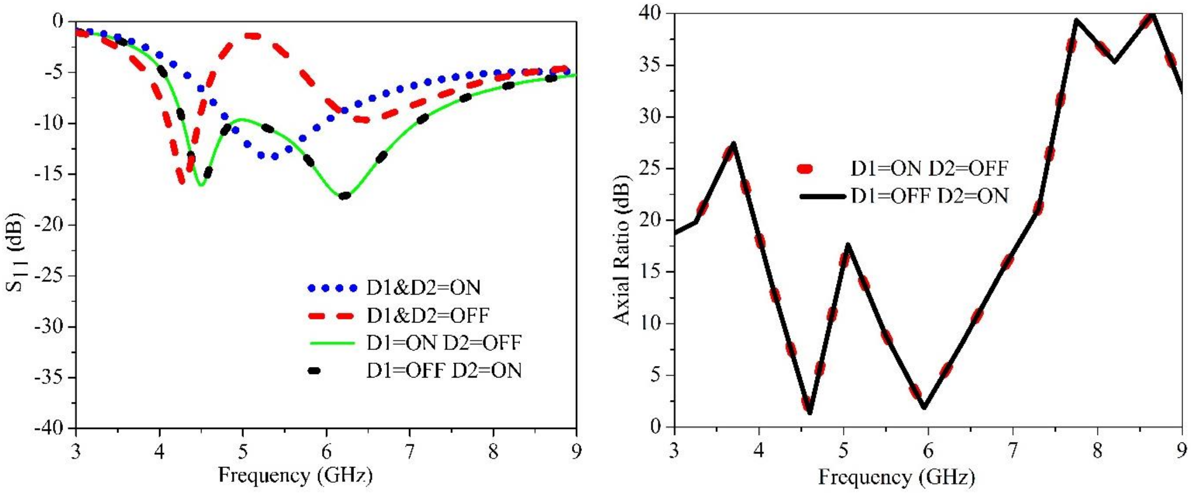

(a) (b)

Figure 5: Simulated results of antenna 4 for different states of diodes (a) Impedance Bandwidth

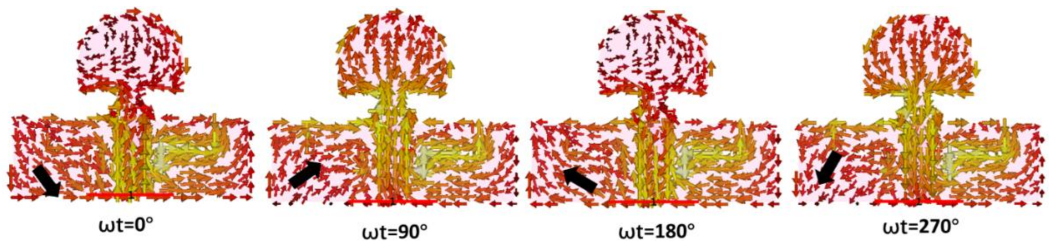

(a)

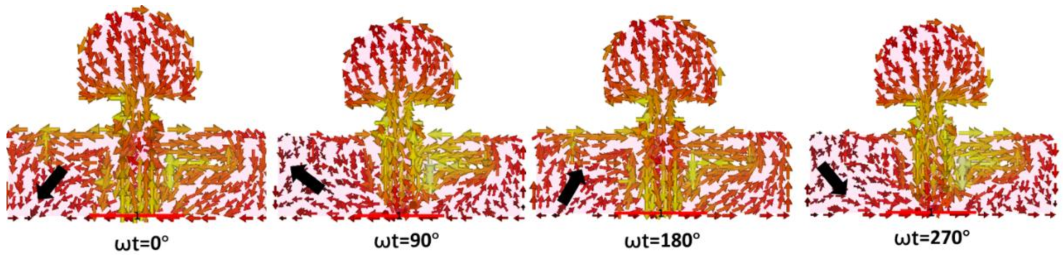

(b)

Figure 6: Simulated surface current distribution of proposed antenna 4 at (a) 4.5 GHz (RHCP) and (b) 6.2 GHz (LHCP) with diode switching states as D1=ON & D2=OFF

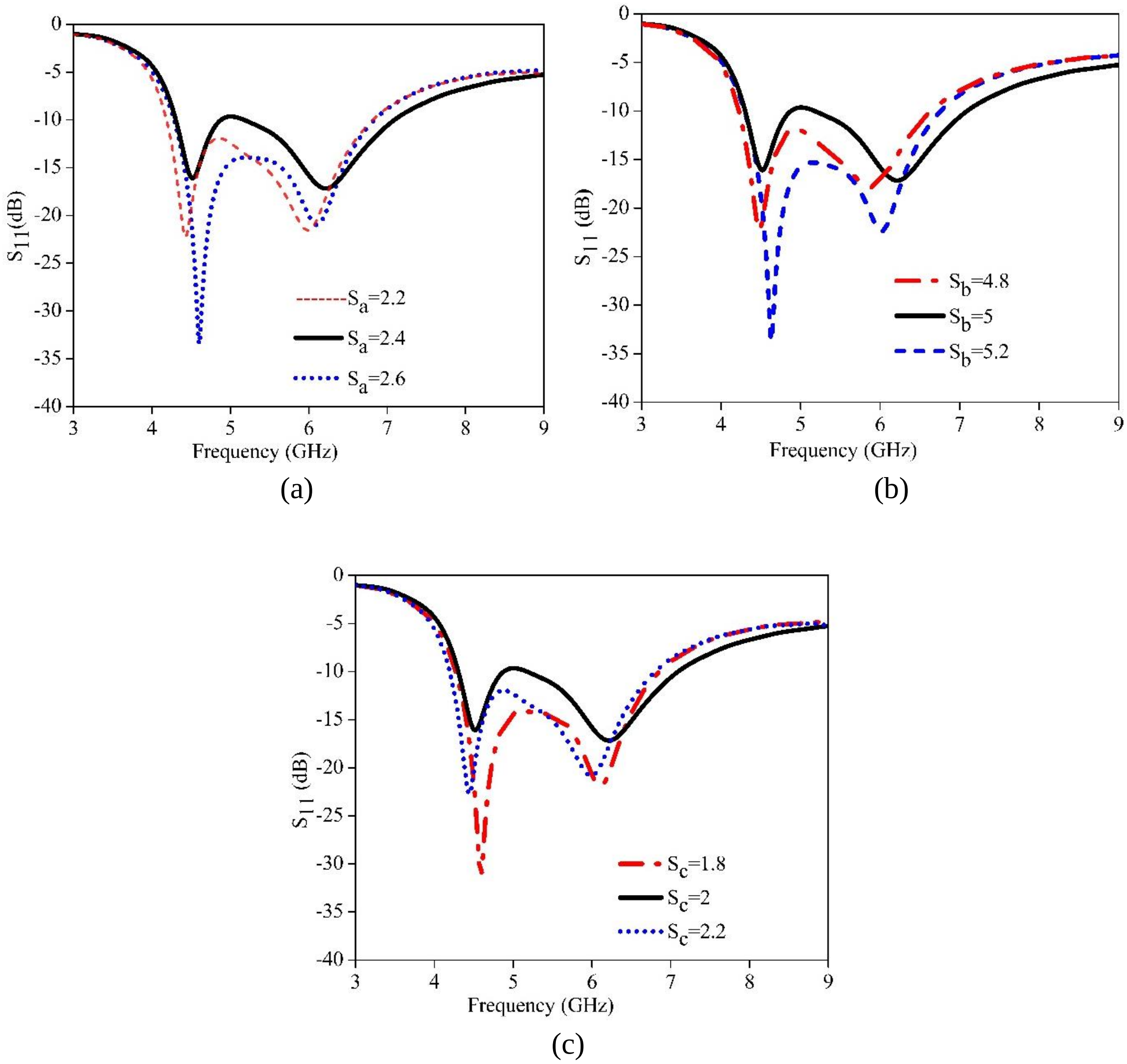

Figure 7: Simulated Impedance Bandwidth of antenna 4 for different values of (a) slit length S_a (b) slit length Sb (c) slit length Sc for D1=ON/OFF &D2=OFF/ON

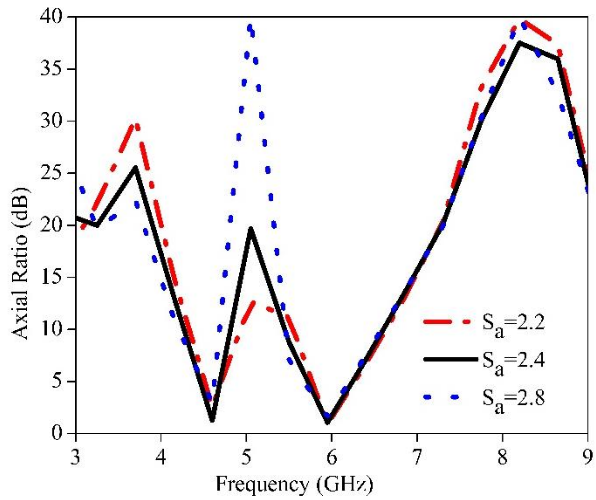

40
35
30
25
20
15
10
5
0
Axial Ratio (dB)
3
4
5
6
7
8
9
Frequency (GHz)
S_a=2.2
S_a=2.4
S_a=2.8

(a)

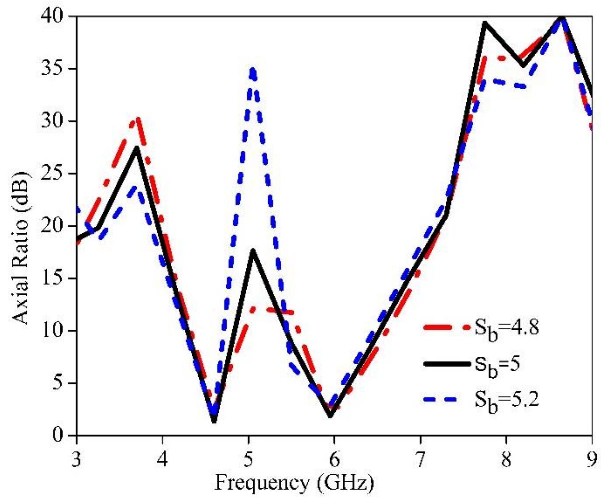

40
35
30
25
20
15
10
5
0
Axial Ratio (dB)
3
4
5
6
7
8
9
Frequency (GHz)
S_b=4.8
S_b=5
S_b=5.2

(b)

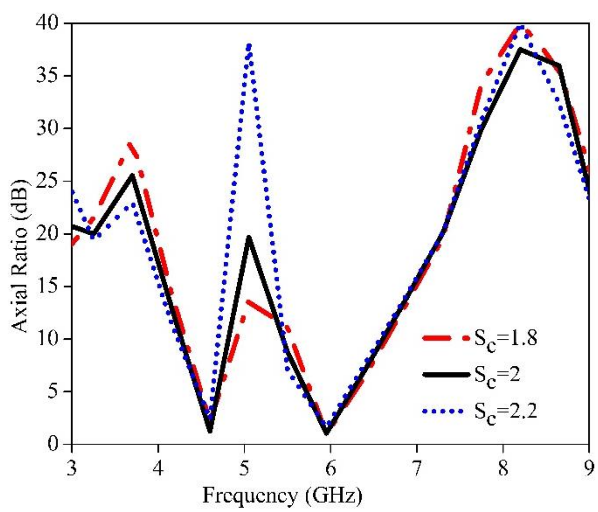

40
35
30
25
20
15
10
5
0
Axial Ratio (dB)
3
4
5
6
7
8
9
Frequency (GHz)
S_c=1.8
S_c=2
S_c=2.2

(c)

Figure 8: Simulated Axial Ratio bandwidth of antenna 4 for different values of (a) slit length S_a (b) slit length S_b (c) slit length S_c for D1=ON/OFF &D2=OFF/ON

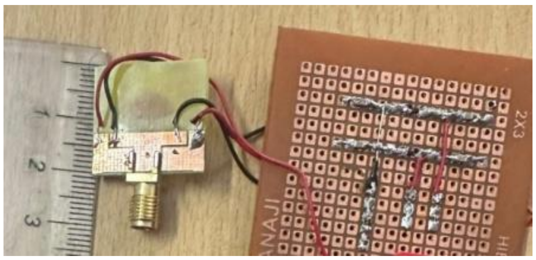

(a) (b)

Figure 9: (a) Antenna with biasing circuit (b) Testing of the suggested antenna in the anechoic chamber

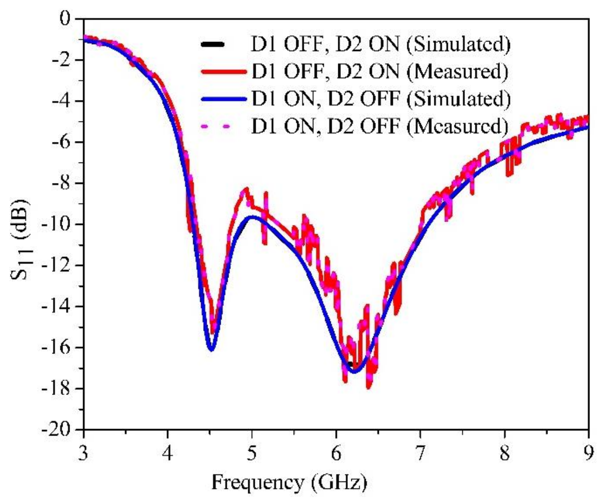

Figure 10: Evaluation of simulated and measured S_{11} for different p-i-n diodes switching states of the suggested antenna

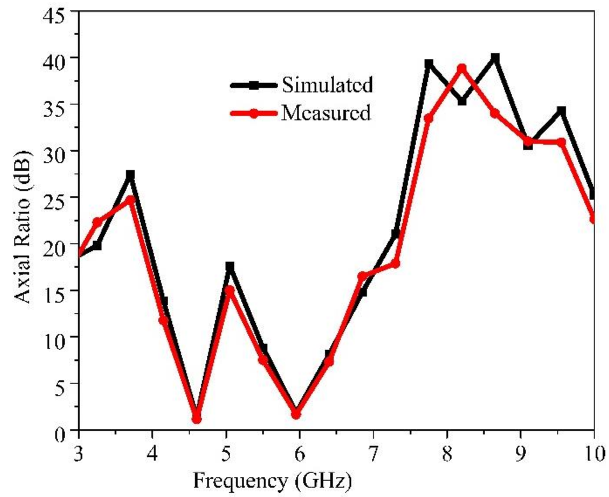

Figure 11: Simulated and measured Axial ratio bandwidth for various switching modes

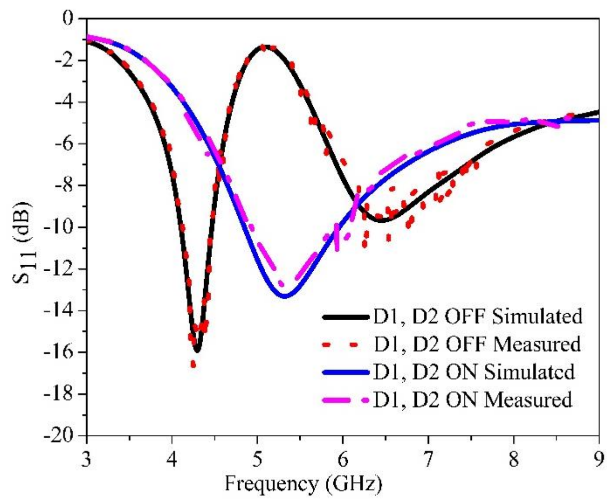

Figure 12: Comparison of simulated and measured IBW of the proposed antenna when both diodes are simultaneously OFF and ON

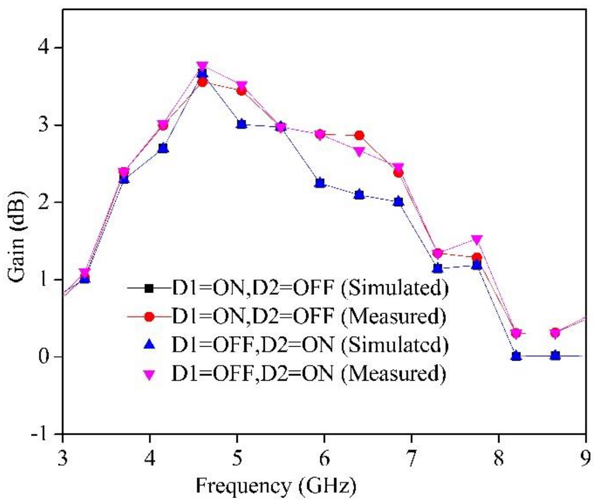

(a)

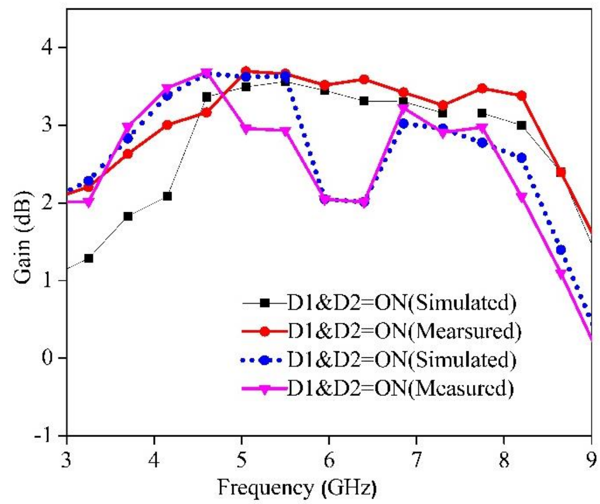

(b)

Figure 13: Comparison of simulated and measured Gain of the designed antenna for different switching states of the diodes (a) D1=ON&D2=OFF/ D1=OFF&D2=ON (b) D1D2=ON/ D1D2=OFF

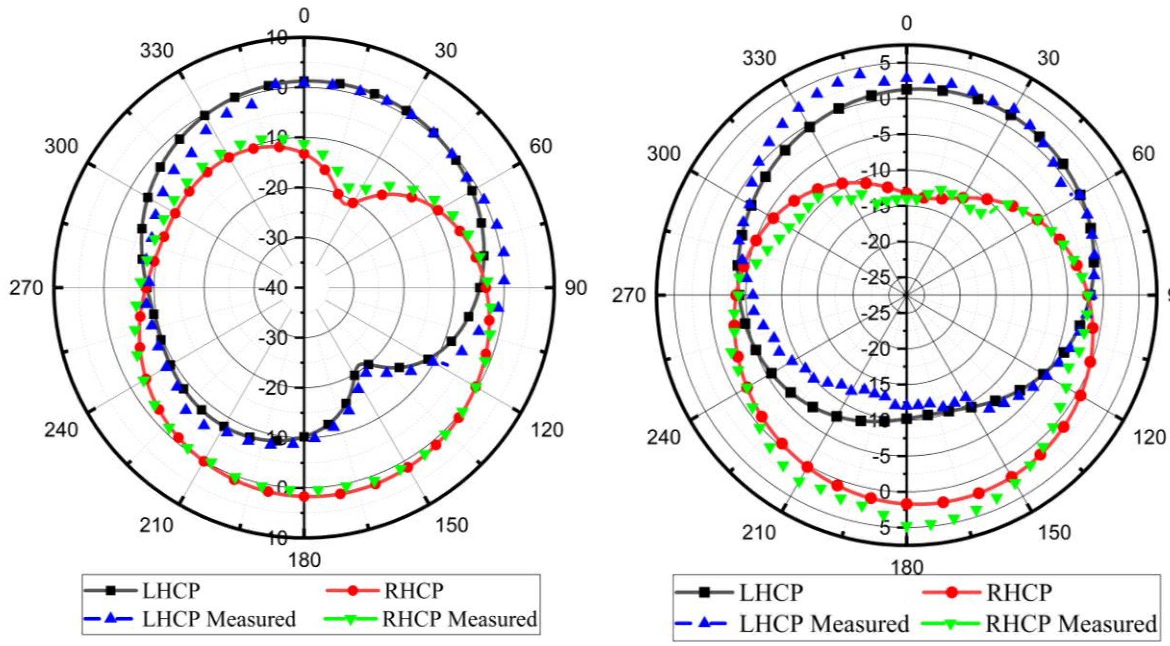

H-plane E-plane

(a)

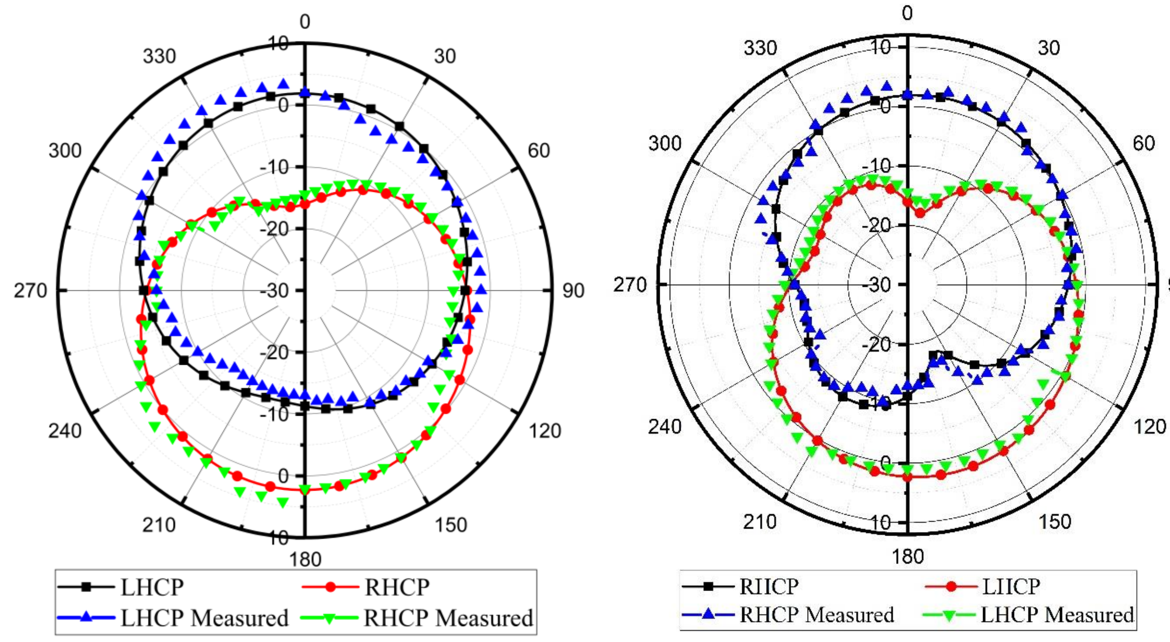

H-plane E-plane

(b)

Figure 14: Simulated and measured radiation pattern of the proposed antenna (a) at 4.5GHz (b) at 6.2 GHz with diode switching D1=OFF& D2=ON when at working as LHCP & RHCP

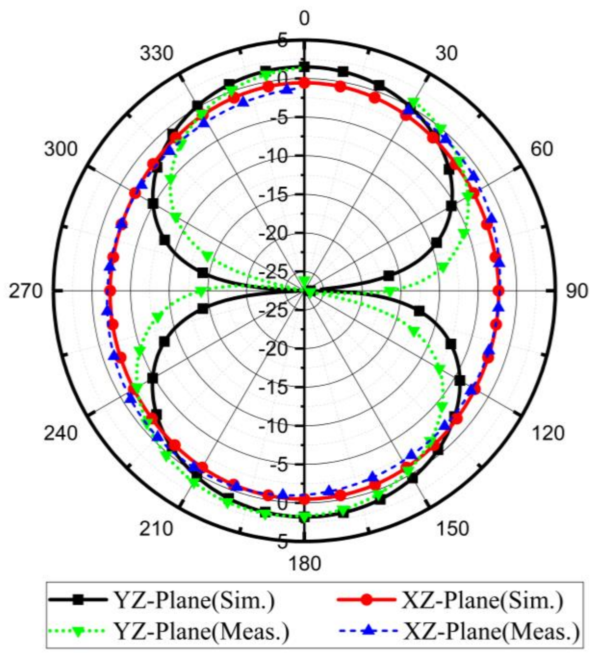

(a)

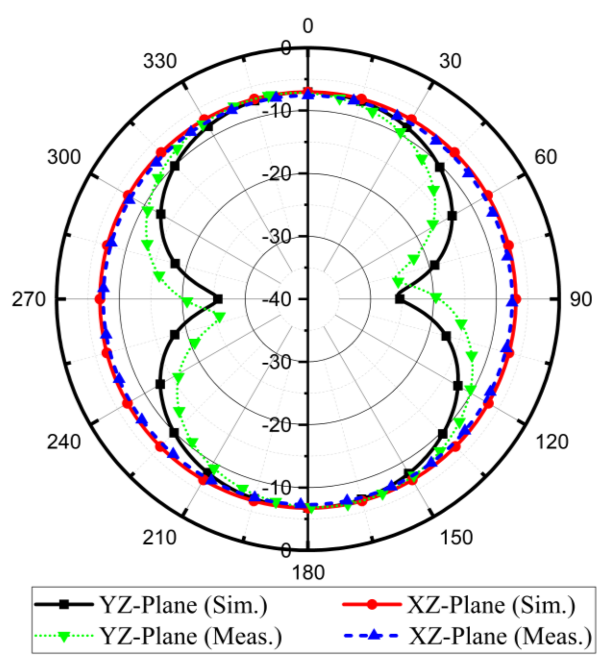

(b)

Figure 15: Simulated and measured radiation pattern of the proposed antenna (a) at 5.3GHz (b) at 4.2 GHz with diode switching D1=ON & D2=OFF

Table 1 Specifications for the suggested antenna's parameters

Parameter	**Value(mm)**	**Parameter**	**Value(mm)**	**Parameter**	**Value(mm)**
L_s	20	R_p	5	S_b	5
W_s	22	L_g	7	S_c	2
W_f	2.1	g	0.4	h	1
L_f	2	$S_x \times S_y$	1x2	S_a	2.4

Table 2 Performance of the suggested antenna for various switching modes of p-i-n diodes

S. No.	**PIN diode state**	**Simulated IBW% (|S_{11}|< -10dB, fo)**	**ARBW%(<3dB)**	**Polarization**	**Band**
1	D1&D2=ON	19.81%(4.9GHz-5.95GHz,5.3GHz)		LP	Single
2	D1&D2=OFF	10%(3.8GHz-4.4GHz,4.2GHz)		LP	Single
3	D1=ON&D2=OFF	12.89%(4.3GHz-4.88GHz,4.5GHz) 29.68%(5.16GHz-7GHz,6.2GHz)	4.56%(4.5GHz-4.71GHz) 8.33%(5.7GHz-6.2GHz)	RHCP LHCP	Dual
4	D1 OFF&D2=ON	12.89%(4.3GHz-4.88GHz,4.5GHz) 29.68%(5.16GHz-7GHz,6.2GHz)	4.56%(4.5GHz-4.71GHz) 8.33%(5.7GHz-6.2fGHz)	LHCP RHCP	Dual

Table 3 Comparative study of the proposed antenna with earlier designed dual band antenna**s**

References	**Size (mm)**	**No of Diodes**	**IBW (%)**	**ARBW(%)**	**Polarization**

[4]	.5λo×.4λo×.02λ0	One	8.9(LP)	.5(CP)	1 CP
[7]	37.8×40.4×1.6	Four	16.6(RHCP/LHCP)	5.7(RHCP/LHCP)	1 CP
[8]	35×30×1	Four	14.8(LP) 8.4(LP)	1.6/2.6 (RHCP)	1 LP 1 CP
[9]	65 ×65 ×.6	Two	4.08	4.08	1 LP 2 CP
[15]	.56λo×.56λo×.037λ0	Four	7.5(LP) 7.1(RHCP/LHCP)	6.25(LHCP/RHCP)	1 LP 1 CP
Present work	**20×20×1**	**Two**	**19.81(LP) 10(LP) 12.89(LHCP/RHCP) 29.68(RHCP/LHCP)**	**4.56(LHCP/RHCP) 8.33(RHCP/LHCP)**	**2 LP 2 CP**

Renu Agrawal is a Lecturer in the Department of Electrical Engineering at Gokul Verma Government Polytechnic College, Bharatpur, Rajasthan, India. She received her BE Degree in Electronics & Communication Engineering in 2003 from Mody College of Engineering & Technology, Lakshmangarh, Sikar, Rajasthan, India. She completed her M.Tech. in VLSI Design from Malaviya National Institute of Technology, Jaipur, Rajasthan, India 2009. Presently, she is pursuing a PhD in Micro-Strip Patch Antenna Design from Malaviya National Institute of Technology (MNIT), Jaipur, Rajasthan, India.

Subhash Shrimal received a B.E. degree in Electronics and communication engineering from the University of Rajasthan, Jaipur, India, in 2005 and an M.Tech. degree in Electronics and communication engineering from Malviya National Institute of Technology, Jaipur, India, in 2008. He has been working toward his PhD (Part-Time) at MNIT Jaipur since 2020. He works as a Lecturer at Government Polytechnic College, Board of Technical Education Rajasthan. His main areas of interest are microstrip and reconfigurable planar antennas.

Bhawna Kalra (Member IEEE) received a B.Tech. degree from RTU Kota in 2013, a master's degree from UCE RTU Kota in 2016, and Pursuing a Ph.D. from MNIT Jaipur. She is currently working as an assistant professor in JECRC Foundation Jaipur. Her area of research includes circularly polarized patch antenna, shared aperture antenna, phased array antenna and antennas for 5G applications.

Mahendra Mohan Sharma received a BE degree in 1985 from NIT, Srinagar, India. He did an M.Tech. from IIT, Delhi, and PhD from MNIT, Jaipur, India. He joined as a Lecturer in the Department of Electrical Engineering, MNIT, Jaipur, in 1986 and was designated as an Associate Professor there in 1995. Presently, He is working as a Professor with the Department of Electronics and Communication Engineering, MNIT Jaipur, besides being an able academician and administrator (Registrar in MNIT and Ex Executive Director at National Institute of Electronics and Information Technology, Chandigarh). He is an active member of IEEE, Broadcasting Engineering Society (India), and a Life Senior Member of ISTE professional bodies. He is the Honorary Secretary of the IEEE-MTTS India Council Chapter. He is the author/co-author of more than 100 research papers published in international/national journals and conferences. His research interests include designing and modeling antennas, array, and FSS.